Polarized backlight based on selective total internal reflection at microgrooves

Ko-Wei Chien, Han-Ping D. Shieh, and Hugo Cornelissen

A polarized backlight for LCD illumination is designed and fabricated in which *s*-polarized light is extracted owing to selective total internal reflection at microstructures in the anisotropic layer. From the measurement, the contrast ratio in normal viewing direction can be as high as 64. Luminous uniformity of higher than 80% is achieved for polarized backlights. Furthermore, 1.6 gain in efficiency is obtained aiming for high-efficiency LCD illumination. © 2004 Optical Society of America

OCIS codes: 240.5420, 260.1440, 160.3710, 150.2950.

1. Introduction

In a conventional backlight for LCD illumination, over 50% of the energy is absorbed in the back polarizer while polarized light is produced. Polarized backlights are more efficient than conventional backlights because they recycle light of undesired polarized direction. In addition, the back polarizer can be left out to further reduce the thickness of LCD modules. In a previous design,[1] a polarized backlight used microstructures at the Brewster angle to produce unipolarized light. However, the polarization efficiency is strongly dependent on the incident angles of light. In addition, a stack of multilayered thin films (alternating layers of materials of high and low refraction indices) was designed to match a quarter-wave optical thickness in each layer, so that Brewster condition was satisfied to produce a specific polarized state of light.[2] However, the tolerances in the incident angle and the wavelength are very limited.

Polarization backlight based on selective total internal reflection (TIR) at the interface of microstructures was proposed.[3] As schematically shown in Fig. 1, a birefringent layer with microgrooves was filled with an isotropic index-matching layer adhering to the lightguide substrate. The birefringent layer has an ordinary index of refraction n_o, which is closely matched to the refraction index of index-matching layer and an extraordinary refraction index n_e. The approach to separate the polarized light was aimed to extract one polarization state of light by selective TIR at the microstructure interface. The extraordinary refractive index n_e of the birefringent layer should be significantly larger than the refractive index n_c of the index-matching layer so that sufficiently small critical angle at the interface can be achieved. In contrast, the critical angle at the interface is not present for the orthogonally polarized light. Light therefore remains in its propagating direction at the interface of the microstructures.

2. Theory

The electric field amplitude E can be decomposed either parallel or perpendicular to the incident plane. The transmission coefficient t and reflection coefficient r depend on the incident polarization direction and are given by the Fresnel equations for dielectric media:[4,5]

TE (s polarization):

$$t = \frac{E_t}{E} = \frac{2 \cos \theta_i}{\cos \theta_i + (n^2 - \sin^2 \theta_i)^{1/2}},$$

TM (p polarization):

$$t = \frac{E_t}{E} = \frac{2n \cos \theta_i}{n^2 \cos \theta_i + (n^2 - \sin^2 \theta_i)^{1/2}},$$

K.-W. Chien and H.-P. D. Shieh (hpshieh@mail.nctu.edu.tw) are with the Institute of Electro-Optical Engineering, National Chiao Tung University, Hsinchu, Taiwan 30010. H. Cornelissen is with Philips Research Laboratories WY63, Professor Holstlaan 4, 5656AA Eindhoven, The Netherlands.

Received 30 March 2004; revised manuscript received 11 May 2004; accepted 17 May 2004.

0003-6935/04/244672-05$15.00/0

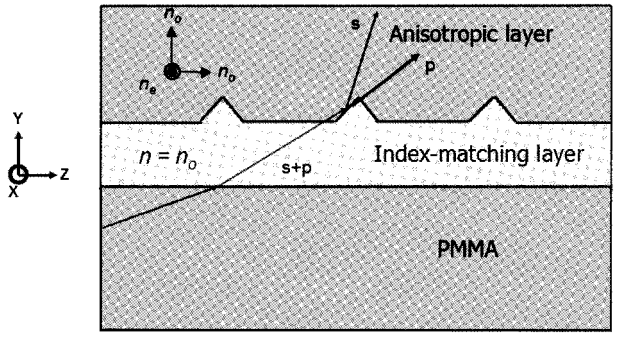

Fig. 1. Schematics of polarized backlight. Birefringent layer with microgrooves filled with index-matching layer was aimed to extract the *s*-polarized light at the interface. Additionally, *p*-polarized light was trapped in the polymethyl methacrylate (PMMA) lightguide to be recycled.

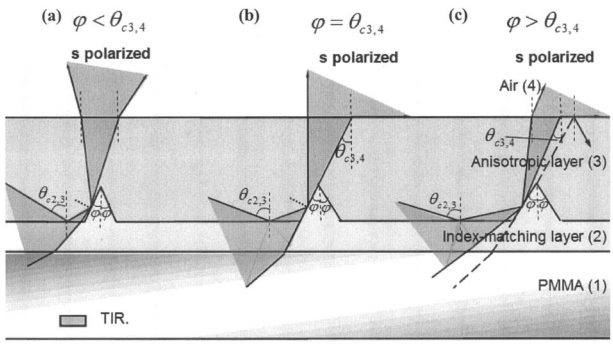

Fig. 2. Illustration of outcoupled *s*-polarized light due to selective TIR at the interface for different half-top angles relative to the critical angle $\theta_{c3,4}$ of the anisotropic layer with respect to air: (a) $\phi < \theta_{c3,4}$, (b) $\varphi = \theta_{c3,4}$, (c) $\varphi > \theta_{c3,4}$.

TE (*s* polarization):

$$r = \frac{E_r}{E} = \frac{\cos\theta_i - (n^2 - \sin^2\theta_i)^{1/2}}{\cos\theta_i + (n^2 - \sin^2\theta_i)^{1/2}},$$

TM (*p* polarization):

$$r = \frac{E_r}{E} = \frac{n^2\cos\theta_i - (n^2 - \sin^2\theta_i)^{1/2}}{n^2\cos\theta_i + (n^2 - \sin^2\theta_i)^{1/2}},$$

in which n is the relative refractive index (n_2/n_1).

The transmittance T and reflectance R are related to the transmission and reflection coefficients by[4,5] $T = n(\cos\theta_t/\cos\theta_i)t^2$ and $R = r^2$.

The above-mentioned Fresnel equations show a polarization dependence of the transmittance and the reflectance at the interface. As shown in Fig. 1, for an uniaxial birefringent film, *p*-polarized light encounters the low ordinary refractive index n_o and *s*-polarized light encounters a weighted average of n_o and n_e. The polarization separation can be achieved at the interface by a complete reflection of one polarization direction, whereas the orthogonal polarization direction is refracted toward the anisotropic film. Only *s*-polarized light encounters TIR, because a critical angle $\theta_c = \sin^{-1}(n_o/n_{\text{effective},s\text{-polarized}})$ exits at the interface, where it is extracted from the lightguide. The angular distributions of outcoupling *s*-polarized light depend on the top angle of microgrooves in the anisotropic layer. Figure 2 demonstrates the distributions of *s*-polarized light if half of the top angle φ is smaller, equal, or exceeding the critical angle $\theta_{c3,4}$ of the anisotropic layer with respect to air.[6] $\theta_{c2,3}$ depicts the critical angle of the anisotropic layer with respect to the index-matching layer. For φ equal to or exceeding $\theta_{c3,4}$, light can be refracted at a maximum external outcoupling angle of 90° if the incident angle is no more than $\theta_{c3,4}$ at the interface between the anisotropic layer and air. Light undergoes TIR and is trapped in the lightguide if the incident angle is larger than $\theta_{c3,4}$. For φ smaller than $\theta_{c3,4}$, light can be refracted at an external outcoupling angle of less than 90°.

3. Simulation

To consider contrast ratio, angular distributions, and efficiency in more detail, we analyzed several issues. An optical simulation and analysis program, Advanced System Analysis Program, was used to simulate the polarized light by Monte Carlo ray tracing in birefringent material. Uniaxial birefringent materials, stretched polyethylene terephthalate (PET) and polyethylene naphthalate (PEN), were used as an anisotropic layer, which was adhered to a polymethyl methacrylate (PMMA) substrate by an index-matching glue. Furthermore, in order to analyze both *s*-polarized and *p*-polarized light, we built a polarizer on the top of polarized backlight model. *s*-polarized light was analyzed when the direction of polarizer was parallel to the direction of microgrooves. p-polarized light was analyzed when the direction of polarizer was perpendicular to the direction of microgrooves. The refractive indices of PMMA and anisotropic layer are listed as

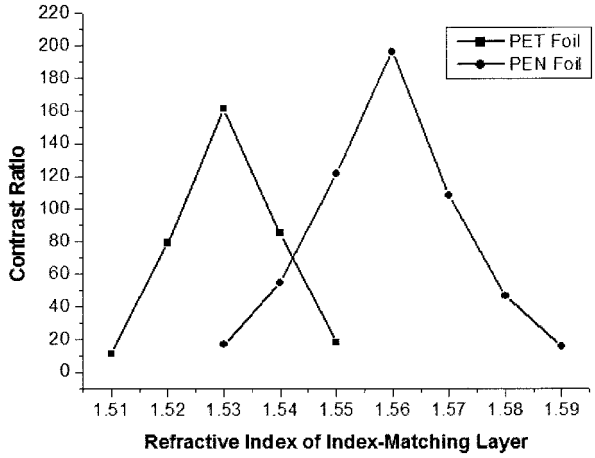

Fig. 3. Illustration of contrast ratio at a different refractive index of index-matching layer. Contrast ratio achieves maximum at perfectly matched refractive index $n = 1.53$ for PET foil, whereas $n = 1.56$ for PEN foil.

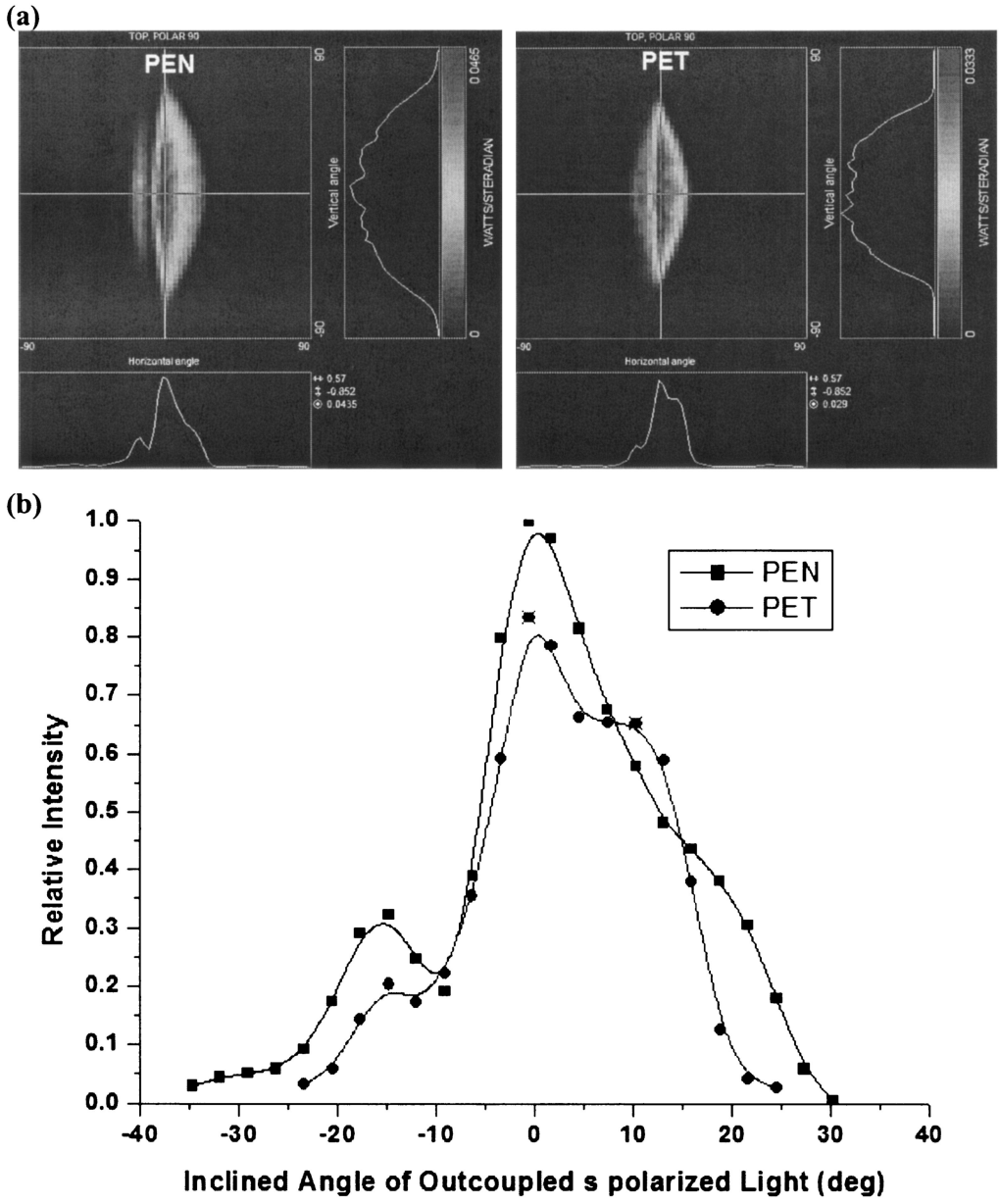

Fig. 4. (a) Angular distributions and (b) Inclined angular cross-sections of outcoupled *s*-polarized light at perfectly matched index for PEN and PET foils, respectively.

(i) PET: $n_{\mathrm{PMMA}} = 1.49$; $n_{o,\mathrm{PET}} = 1.53$; $n_{e,\mathrm{PET}} = 1.71$,
(ii) PEN: $n_{\mathrm{PMMA}} = 1.49$; $n_{o,\mathrm{PEN}} = 1.56$; $n_{e,\mathrm{PEN}} = 1.86$.

Contrast ratio of the polarized backlight model was analyzed at different refractive indices of the index-matching layer. Contrast ratio is defined as the ratio of intensity of *s*-polarized to *p*-polarized light. For PEN foil, contrast ratio achieves 190 at perfectly matched $n = 1.56$, whereas 160 is achieved at $n = 1.53$ for PET foil, shown in Fig. 3.

As shown in Fig. 4, we demonstrated the angular distributions and inclined angular cross sections of outcoupling *s*-polarized light at perfectly matched indices for PEN and PET foils, respectively. The top angle of grooves is 50°. The angular profiles are plotted as a function of inclination angles, which range from −90° to 90°, with respect to the normal viewing direction. Most of the *s*-polarized light is distributed between the inclination angle of −30° and 30° for PEN foil and −25° and 25° for PET.

4. Experiments

Stretched PEN foils were adhered to a PMMA substrate by UV curing of the index-matching glue. Microgrooves were directly cut into PEN foils by diamond turning. The top angle and the depth of the grooves were 50° and 56.5 μm, respectively. The pitch of the grooves was 200 μm. The polarized

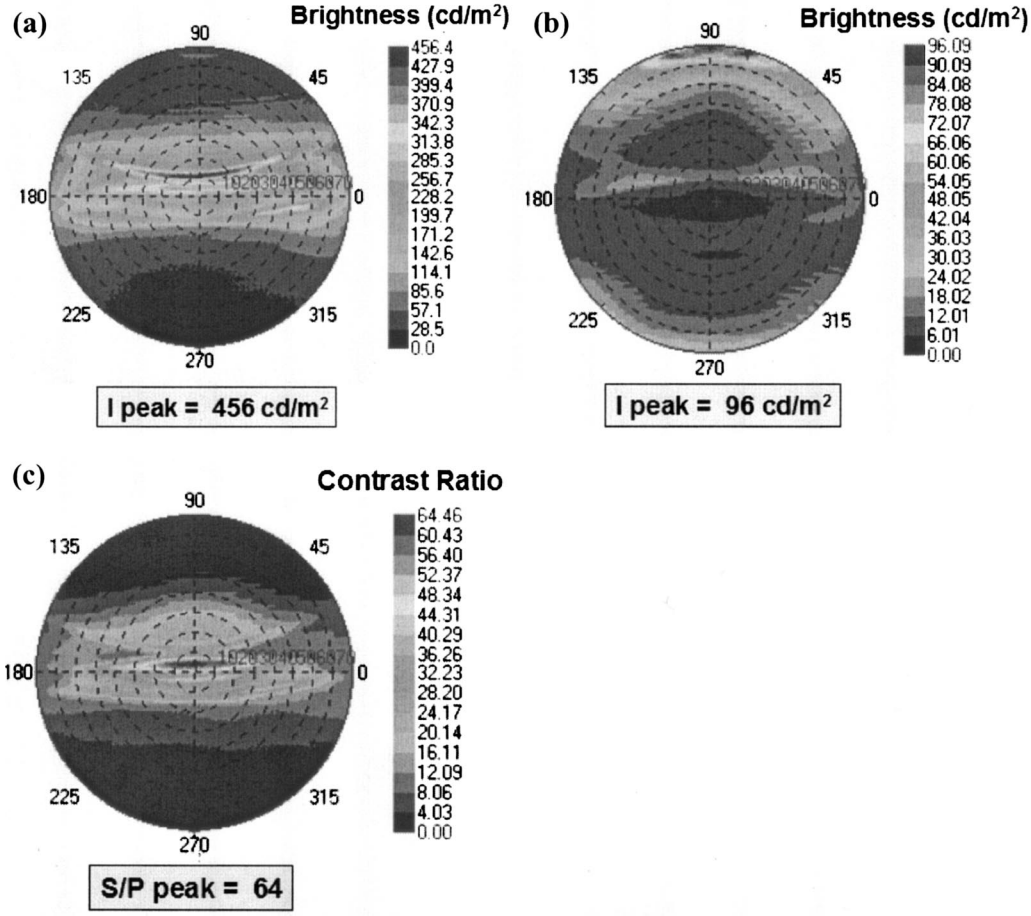

Fig. 5. Measured angular profiles of (a) *s*-polarized light and (b) *p*-polarized light and (c) contrast ratio of *s*-polarized to *p*-polarized light.

backlight module was side illuminated by a cold-cathode fluorescent lamp. Angular distributions of emitting light from the backlight module were measured with an EZcontrast 160 measuring system. To determine the contrast ratio of *s*-polarized light to *p*-polarized light, we placed a polarizer between the backlight and the detector, so that the transmission axis of polarizer could be rotated to be parallel or perpendicular to the extraordinary axis of the birefringent layer. Figures 5(a) and 5(b) demonstrated the angular distributions of *s*-polarized and *p*-polarized light, respectively, where the angular distributions were plotted as a function of azimuth angle ϕ' ranging from 0° to 360°, and the inclination angle

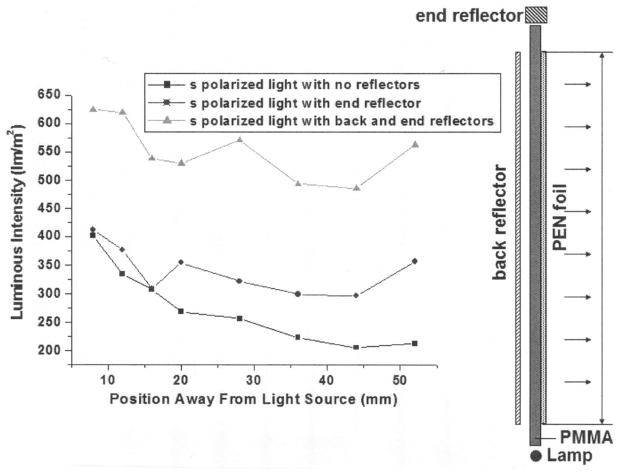

Fig. 6. For PEN foil adhered on the substrate of PMMA, luminous intensity versus position from light source. Squares, circles, and triangles illustrate luminous intensity of *s*-polarized light with no reflectors, diffuse end reflector only, and both back and end reflectors, respectively.

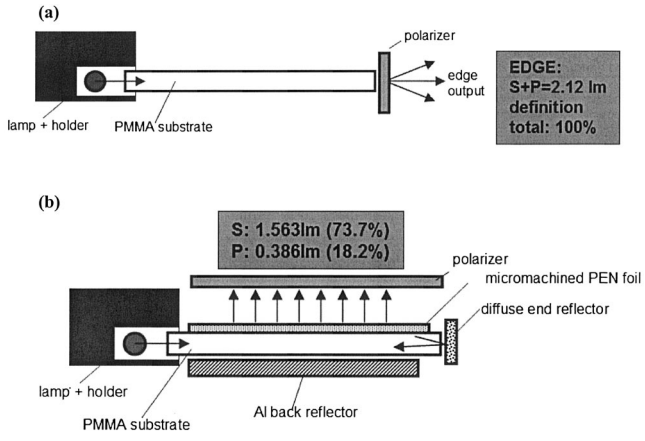

Fig. 7. Measurement set up of flux by (a) clear PMMA and (b) polarized backlight with both back and end reflectors.

θ, ranging from 0° to 80°. Peak intensity is 456 cd/m^2 for the *s*-polarized light and 96 cd/m^2 for the *p*-polarized light. Most *s*-polarized light is distributed between the inclination angle of −30° and 30°. *p*-polarized light is distributed in large inclination angles. Figure 5(c) depicts the contrast ratio of *s*-polarized light to *p*-polarized light. The peak value of contrast ratio of *s*-polarized to *p*-polarized light achieves 64.

From the measured results, it is clear that *s*-polarized light significantly dominates the emitting light of the polarized backlight module. However, because the scattering light occurred at the surfaces of the microgrooves, the contrast ratio of *s*-polarized to *p*-polarized light is not yet sufficiently high. We expect that the contrast ratio can be further enhanced when the surface smoothness of the microgrooves is improved. Additionally, luminous intensity was sequentially measured from a position of 8 mm away from the light source (i.e., close to the light source) to a position of 52 mm away from the light source (i.e., far away from light source). As shown in Fig. 6, curves with squares, circles, and triangles illustrate the luminous intensity of the *s*-polarized light with no reflectors, diffuse end reflector only, and both back and end reflectors, respectively. With both back reflector and end reflector, the maximum and the minimum of luminous intensity are 625 and 500 lm/m^2, respectively. Uniformity can therefore reach 80%.

To evaluate the gain of efficiency of polarized backlight, we measured the efficiency by following procedures shown in Fig. 7. Total input flux was measured at the end of a clear PMMA. Theoretically, all of the rays were TIR in the lightguide until being transmitted through the end. Therefore total input flux was 2.12 lm. Then, fluxes of *s*-polarized and *p*-polarized light were sequentially measured to be 1.56 and 0.39 lm, respectively, from the outcoupled plane. Input fluxes of *s*-polarized and *p*-polarized light were assumed to be equally 0.975 lm [(1.56 lm + 0.39 lm)/2 = 0.975 lm]. Outcoupled energy was totally 92% of input flux. The rest 8% flux was lost in reflectors and lamp. Therefore, an efficiency gain factor of 1.6 was achieved for *s*-polarized light (gain factor = 1.56 lm/0.975 lm = 1.6).

5. Discussion

Compared with PET foil, stretched PEN foil demonstrates a higher contrast ratio of *s*-polarized to *p*-polarized light owing to large difference of refractive indices ($\Delta n = n_{e,\mathrm{PEN}} - n_{o,\mathrm{PEN}} = 0.3$, $\Delta n = n_{e,\mathrm{PET}} - n_{o,\mathrm{PET}} = 0.18$). Additionally, PEN demonstrates a wider angular distribution than does PET owing to the large birefringence. Most of the *s*-polarized light is distributed between the inclination angle of −30° and 30° for PEN foil and −25° and 25° for PET. A smaller critical angle is presented at the interface of grooves for PEN, thus broadening the angular distribution on the outcoupled plane. In simulation, when the ordinary refractive index $n_o = 1.56$ of PEN foil is perfectly matched to the refractive index of glue layer, the flux of the *p*-polarized light is expected to achieve a minimum, whereas for PET foil is perfectly matched at $n_o = 1.53$. Therefore the contrast ratio of *s*-polarized light to *p*-polarized light achieves a maximum. However, the mismatched indices between the anisotropic foil and the glue layer cause an increasing amount of *p*-polarized light owing to Fresnel surface reflection at the interface,[7] but not obviously for *s*-polarized light; thus, the contrast ratio degrades. To retain a contrast ratio of higher than 80, one can mismatch the refractive index of the glue layer to within ±0.015 for the PEN foil and ±0.01 for the PET foil. Therefore the PEN foil provides higher tolerances in mismatched refractive indices compared with the PET foil. However, from the measured results, the contrast ratio is lower than our designed value because of the presence of dust and air bubbles during the process of micromachining the anisotropic foil and the index-matching glue. The contrast ratio can be further increased by a more-controllable fabrication process.

6. Conclusion

A polarized backlight based on selective TIR at the interface of microgrooves was demonstrated. An outcoupling of *s*-polarized light occurs in a cone of ±30° around the surface normal, whereas *p*-polarized stray light occurs in large inclination angles. Contrast ratio in normal viewing direction can be as high as 64. Additionally, polarized backlights with end and back reflectors provide luminous uniformity of higher than 80%. Furthermore, a 1.6 gain in efficiency is obtained, aiming for high-efficiency LCD illumination.

References

1. M. F. Weber, "Retroreflecting sheet polarizer," in *Society for Information Display International Symposium Digest*, J. Morreale, ed. (Society for Information Display, San Jose, Calif., 1992), pp. 427–429.
2. Z. Pang and L. Li, "Novel high efficiency polarizing backlighting system with a polarizing beam splitter," in *Society for Information Display International Symposium Digest*, J. Morreale, ed. (Society for Information Display, San Jose, Calif., 1999), pp. 916–919.
3. H. Jagt, H. Cornelissen, D. Broer, and C. Bastiaansen, "Microstructured polymeric linearly polarized light-emitting lightguide for LCD illumination," in *Society for Information Display International Symposium Digest*, J. Morreale, ed. (Society for Information Display, San Jose, Calif., 2002), pp. 1236–1239.
4. E. Hecht, *Optics*, 2nd ed. (Addison-Wesley, Reading, Mass., 1987), p. 84.
5. F. J. Pedrotti and L. S. Pedrotti, *Introduction to Optics*, 2nd ed. (Prentice Hall, London, 1993), p. 38.
6. H. Jagt, *Polymeric Polarisation Optics for Energy Efficient Liquid Crystal Display Illumination* (University Press Facilities, Eindhoven, The Netherlands, 2001), p. 114.
7. G. R. Fowles, *Introduction to Modern Optics*, 2nd ed. (Holt, Rineheart & Winston, New York, 1975), p. 168.